

1 Hydroxyl carlactone derivatives are predominant strigolactones in *Arabidopsis*

2

3 Kaori Yoneyama^{1,2#}, Kohki Akiyama³, Philip B. Brewer⁴, Narumi Mori³, Miyuki Kawada¹,
4 Shinsuke Haruta¹, Hisashi Nishiwaki¹, Satoshi Yamauchi¹, Xiaonan Xie⁵, Mikihisa Umehara⁶,
5 Christine A. Beveridge⁷, Koichi Yoneyama^{5,8} and Takahito Nomura⁵

6

7 ¹Graduate School of Agriculture, Ehime University, Matsuyama 790-8566, Japan; ²PRESTO,
8 Japan Science and Technology, Kawaguchi, Saitama 332-0012, Japan; ³Department of
9 Applied Life Sciences, Graduate School of Life and Environmental Sciences, Osaka
10 Prefecture University, Sakai, Osaka 599-8531, Japan; ⁴ARC Centre of Excellence in Plant
11 Energy Biology, School of Agriculture, Food and Wine, The University of Adelaide, Glen
12 Osmond, SA 5064, Australia; ⁵Center for Bioscience Research and Education, Utsunomiya
13 University, Utsunomiya 321-8505, Japan; ⁶Department of Applied Biosciences, Faculty of
14 Life Sciences, Toyo University, Gunma 374-0193, Japan; ⁷ARC Centre of Excellence for
15 Plant Success in Nature and Agriculture, School of Biological Sciences, The University of
16 Queensland, St. Lucia, QLD 4072, Australia; ⁸Women's Future Development Center, Ehime
17 University, Matsuyama 790-8577 Japan

18

19 # Author for correspondence:

20 Kaori Yoneyama

21 Tel: +81 89 946 9851

22 Email: yoneyama.kaori.wx@ehime-u.ac.jp

23

24

25

26 Author contributions

27

28 Kaori Yoneyama, K.A., Koichi Yoneyama, and T.N. designed the research; Kaori Yoneyama,

29 K.A., N.M., X.X., and P.B. performed research; Kaori Yoneyama, K.A., H.N., S.H., S.Y.,

30 M.U., and C.B. analyzed data; and Kaori Yoneyama, K.A, P.B., and Koichi Yoneyama wrote

31 the manuscript.

32

33 **ABSTRACT**

34

35 Strigolactones (SLs) regulate important aspects of plant growth and stress responses. Many
36 diverse types of SL occur in plants, but a complete picture of biosynthesis remains unclear. In
37 *Arabidopsis thaliana*, we have demonstrated that MAX1, a cytochrome P450
38 monooxygenase, converts carlactone (CL) into carlactonoic acid (CLA), and that LBO, a
39 2-oxoglutarate-dependent dioxygenase, converts methyl carlactonoate (MeCLA) into a
40 metabolite called [MeCLA+16] Da. In the present study, feeding experiments with deuterated
41 MeCLAs revealed that [MeCLA+16] Da is hydroxymethyl carlactonoate (1'-HO-MeCLA).
42 Importantly, this LBO metabolite was detected in plants. Interestingly, other related
43 compounds, methyl 4-hydroxycarlactonoate (4-HO-MeCLA) and methyl
44 16-hydroxycarlactonoate (16-HO-MeCLA) were also found to accumulate in *lbo* mutants.
45 3-HO-, 4-HO- and 16-HO-CL were detected in plants, but their expected corresponding
46 metabolites, HO-CLAs, were absent in *max1* mutants. These results suggest that HO-CL
47 derivatives are predominant SLs in *Arabidopsis*, produced through MAX1 and LBO.

48

49 Key words: *Arabidopsis thaliana*, hydroxyl carlactone derivative, lateral branching
50 oxidoreductase.

51

52 INTRODUCTION

53

54 Strigolactones (SLs) were originally identified as germination stimulants for root parasitic
55 plants (Cook et al., 1966) and then as hyphal branching factors for symbiotic arbuscular
56 mycorrhizal (AM) fungi (Akiyama et al., 2005). SLs were thought to function only as
57 rhizosphere signals until the discovery of their role as a plant hormonal signal that inhibits
58 lateral shoot branching (Gomez-Roldan et al., 2008; Umehara et al., 2008).

59 Shoot branching involves the formation of axillary buds in the axil of leaves. The level of
60 dormancy in buds is an essential determinant of plant architecture. Defects in the SL pathway
61 correspond with loss of bud dormancy and excessive shoot branching as displayed by SL
62 mutants that include *ramosus (rms)* of pea (*Pisum sativum*), *decreased apical dominance*
63 (*dad*) of petunia (*Petunia hybrida*), *dwarf (d)* of rice (*Oryza sativa*) and *more axillary growth*
64 (*max*) of *Arabidopsis (Arabidopsis thaliana)*.

65 Natural SLs are carotenoid-derived compounds consisting of a butenolide D ring linked by
66 an enol ether bridge to a less conserved moiety. These SLs can be classified into two
67 structurally distinct groups: canonical and non-canonical SLs. Canonical SLs contain the
68 ABCD ring formation, and non-canonical SLs lack the A, B, or C ring but have the enol
69 ether-D ring moiety (Al-Babili and Bouwmeester, 2015). During biosynthesis, the initial
70 compound that contains the D ring is carlactone (CL), an endogenous precursor for SLs,
71 which is produced by the sequential reactions of 9-*cis*/all-*trans*- β -carotene isomerase and two
72 carotenoid cleavage dioxygenases (CCD7, CCD8) (Alder et al., 2012). In *Arabidopsis*, the
73 isomerase is encoded by *DWARF27 (D27)*, and CCD7 and CCD8 by *MAX3* and *MAX4*,
74 respectively (Fig. 1). We have demonstrated that recombinant MAX1, (a cytochrome P450
75 monooxygenase) expressed in yeast, converts CL to carlactonoic acid (CLA) by oxidations at
76 C-19 (Abe et al. 2015). This function was also observed in MAX1 homologs of other plant

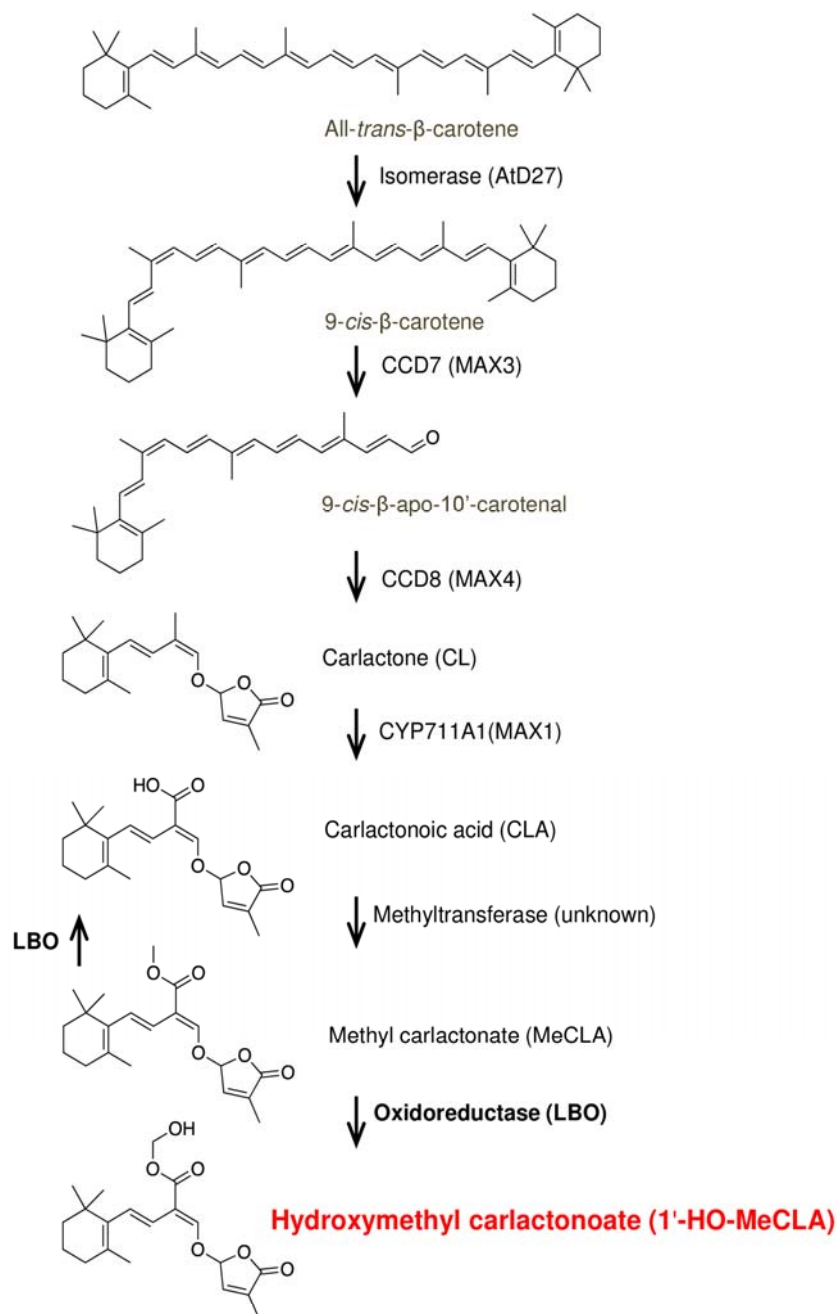


Figure 1. Proposed strigolactone (SL) biosynthesis pathway in *Arabidopsis*. An isomerase (AtD27) and two CCD enzymes (MAX3 and MAX4) convert β -carotene into carlactone (CL), an endogenous common precursor for diverse SLs. CL is then oxidized by cytochrome P450 (MAX1) to carlactonoic acid (CLA), which is converted into MeCLA by unknown methyltransferase. The present study showed that 2-oxoglutarate-dependent dioxygenase LBO converts MeCLA into 1'-HO-MeCLA, which is essential for regulating shoot branching.

77 species including rice, maize, tomato, a model tree poplar, and a lycophyte spike moss,
78 suggesting this conversion of CL to CLA is highly conserved in the plant kingdom

79 (Yoneyama et al., 2018). It was also shown that CL, CLA, and methyl carlactonoate
80 (MeCLA) are present in *Arabidopsis* root tissues (Seto et al., 2014; Abe et al., 2014).
81 Furthermore, differential scanning fluorimetry and hydrolysis activity tests showed that,
82 among CL, CLA, and MeCLA, only MeCLA could interact with the SL receptor, AtD14,
83 suggesting MeCLA may be biologically active in the inhibition of shoot branching in
84 *Arabidopsis* (Abe et al., 2015). *Arabidopsis max1* mutants display a highly increased lateral
85 shoot branching phenotype, and yet accumulate CL (Seto et al., 2014), indicating that CL is
86 not active in repressing shoot branching.

87 As a novel SL biosynthetic gene, *LATERAL BRANCHING OXIDOREDUCTASE (LBO)*,
88 encoding a 2-oxoglutarate and Fe (II)-dependent dioxygenase was identified by using a
89 transcriptomic approach, and was shown to function downstream of MAX1 (Brewer et al.,
90 2016). *Arabidopsis lbo* mutant shoot branching is increased compared to WT (Ws-4), but its
91 phenotype is intermediate between WT and *max4* mutants. LC-MS/MS analysis of SLs
92 revealed that CL and MeCLA accumulate in root tissues of *lbo* mutants (Brewer et al., 2016).
93 Because the active shoot branching inhibitor MeCLA accumulates in *lbo* mutants, the
94 intermediate branching phenotype of *lbo* mutants may be explained by the presence of
95 MeCLA. Thus, it was suggested that LBO is necessary for complete suppression of shoot
96 branching in plants by converting the partly bioactive MeCLA to a compound with greater
97 bioactivity for branching. We then showed that the LBO enzyme expressed in *E. coli* only
98 consumed MeCLA when fed with CL, CLA, or MeCLA, and converted MeCLA into a
99 product of [MeCLA+16] Da. However, complete characterization of this LBO metabolite had
100 not yet been conducted.

101 In the present study, we have determined the structure of the [MeCLA+16] Da compound
102 produced by LBO from MeCLA by feeding experiments using deuterated MeCLAs. In
103 addition, we could identify this LBO metabolite as an endogenous compound from not only

104 roots, but also basal parts of *Arabidopsis* shoot tissues. Since two additional *lbo* mutant
105 alleles, *lbo-2* and *lbo-3*, exist, and homozygous mutant plants exhibited increased shoot
106 branching (Brewer et al., 2016), recombinant proteins of LBO-2 and LBO-3 were produced
107 and the correlation between their enzymatic activities in the conversion of MeCLA to
108 [MeCLA+16] Da and their shoot branching phenotypes was investigated to further examine
109 the importance of the LBO metabolite for shoot branching. Then, biochemical functions of
110 LBO homologs in other plant species including tomato, maize, and sorghum were examined
111 to clarify if the conversion of MeCLA to [MeCLA+16] Da is conserved among these plant
112 species. Furthermore, endogenous SLs in *Arabidopsis max1* and *lbo* mutants were carefully
113 analyzed in search of other potential substrates for MAX1 and LBO to better understand the
114 SL biosynthetic pathway in *Arabidopsis*.

115

116

117 **RESULTS**

118

119 **LBO catalyzes the conversion of methyl carlactonoate (MeCLA) into hydroxymethyl**
120 **carlactonoate (1'-HO-MeCLA)**

121

122 To characterize the structure of [MeCLA+16] Da, LBO enzyme reactions were performed
123 repeatedly. Both the substrate MeCLA and the metabolite [MeCLA+16] Da were highly
124 unstable and the yield of the metabolite was extremely low. We tried to optimize enzyme
125 assay conditions but the maximum yield of the LBO metabolite did not exceed 0.1%.
126 Although more than 500 µg of synthetic MeCLA has been used for LBO enzyme assay, the
127 amount of the metabolite after purification by DEA, silica, and HPLC was not enough for
128 NMR spectroscopy measurement.

129 The observed mass of [MeCLA+16] Da (Brewer et al. 2016) suggests that LBO has simply
130 added an oxygen to MeCLA. Therefore, feeding experiments with using deuterated MeCLAs
131 were conducted to identify the site of oxidation of MeCLA (Nomura et al., 2013). When
132 MeCLA was fed to LBO, the metabolite was detected by the transition of m/z 363 to 97 (Fig.
133 2). When 18- d_3 -MeCLA was fed, the metabolite was detected by the transition of m/z 366 to
134 97 (Fig. 2), clearly indicating that 18- d_3 remained unaffected and thus oxidation did not occur
135 at C-18. By contrast, when 1'- d_3 -MeCLA, in which ester methyl group had been labeled with
136 deuterium was fed, major metabolite was detected by the transition of m/z 365 to 97 (Fig. 2),
137 apparently showing that ester methyl group was oxidized. Consequently, it was demonstrated
138 that LBO converts MeCLA into hydroxymethyl carlactonoate (1'-HO-MeCLA) (Fig. 1).

139 On the other hand, when MeCLA was incubated with LBO, most MeCLA was converted to
140 CLA; the ratio of CLA to 1'-HO-MeCLA was 100: 1 based on the peak areas in the
141 LC-MS/MS chromatograms of LBO reaction products (Fig. 3), indicating that the LBO

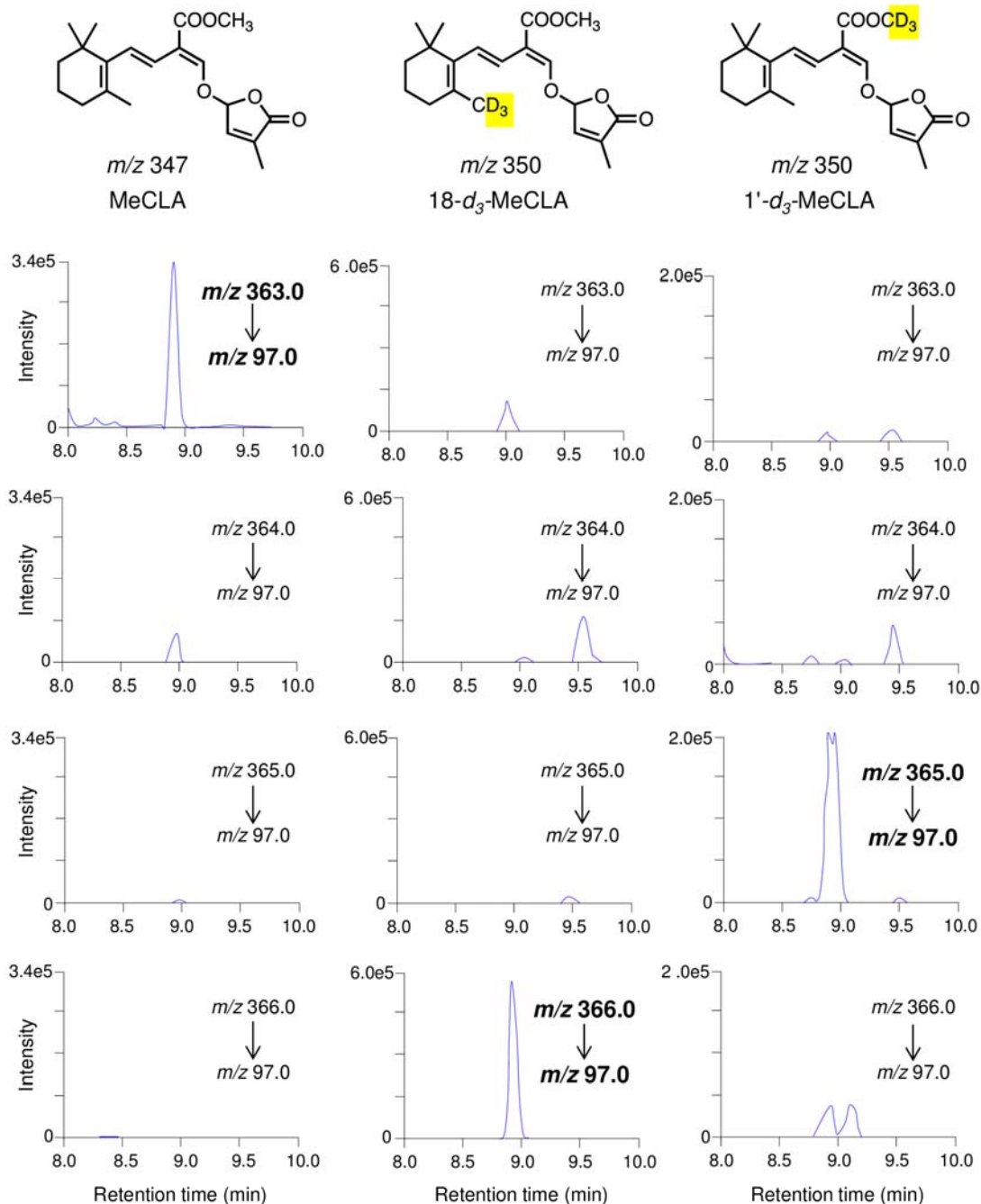


Figure 2. LBO converted $[18-d_3]$ -MeCLA to $[\text{MeCLA}+16+3]$ and $[1'-d_3]$ -MeCLA to $[\text{MeCLA}+16+2]$. To characterize the structure of $[\text{MeCLA}+16]$, $[18-d_3]$ -MeCLA (*Middle*) and $[1'-d_3]$ MeCLA (*Light*) were fed as substrates to recombinant LBO proteins and incubated for 15 min. Products were identified by LC-MS/MS (MRM).

142 protein assay mainly produces CLA.

143

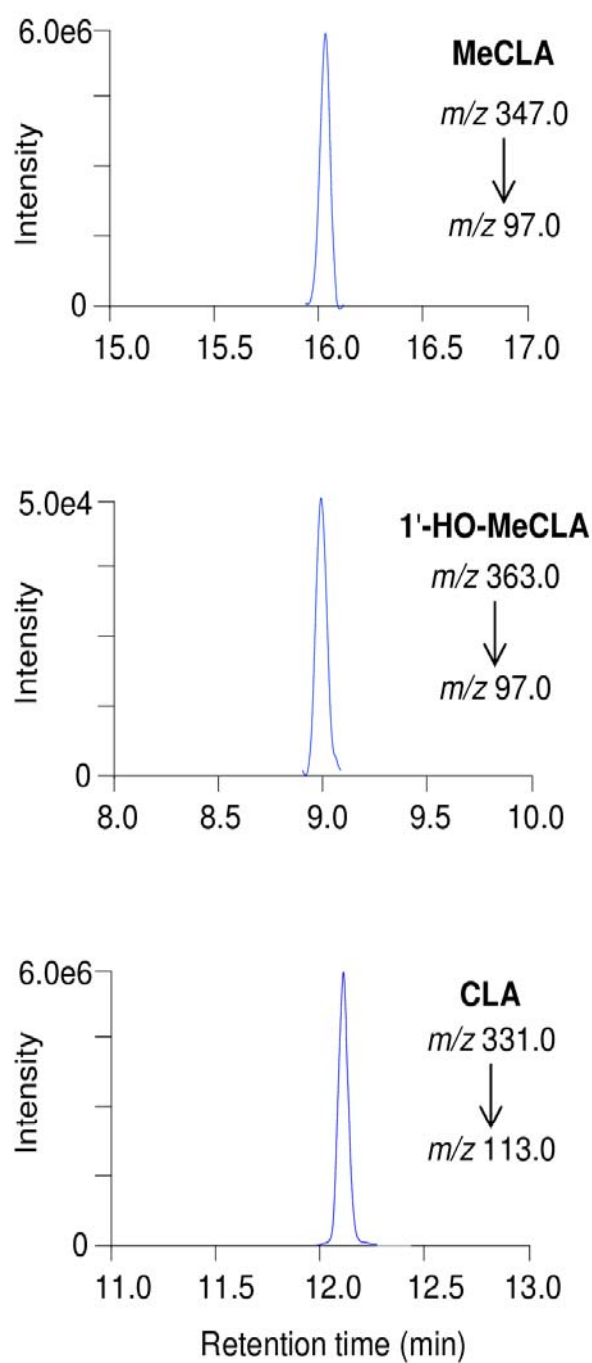


Figure 3. Most MeCLAs were converted to CLA. MeCLA was incubated with recombinant LBO proteins for 15 min. The extracts were analyzed by LC-MS/MS (MRM).

145

146 It is important to clarify if 1'-HO-MeCLA is an endogenous compound in plant tissues
147 because there is a possibility that 1'-HO-MeCLA would only be produced in the heterologous
148 expression system. Identification of 1'-HO-MeCLA was conducted using *atd14* mutant plants,
149 because they lack a functional SL receptor and accumulate SLs due to negative feedback on
150 the biosynthesis pathway. As a negative control, *lbo* mutant plants were also used.
151 1'-HO-MeCLA was detected from the basal part of shoots, and also root tissues of *atd14*
152 mutants (Fig. 4). By contrast, CL and MeCLA, but not 1'-HO-MeCLA, were detected from
153 both tissues of *lbo* mutants (Fig. 4, Brewer et al. 2016). These results clearly indicate that
154 LBO may act to convert MeCLA into 1'-HO-MeCLA in plants.

155

156 **Production of 1'-HO-MeCLA correlates with shoot branching**

157

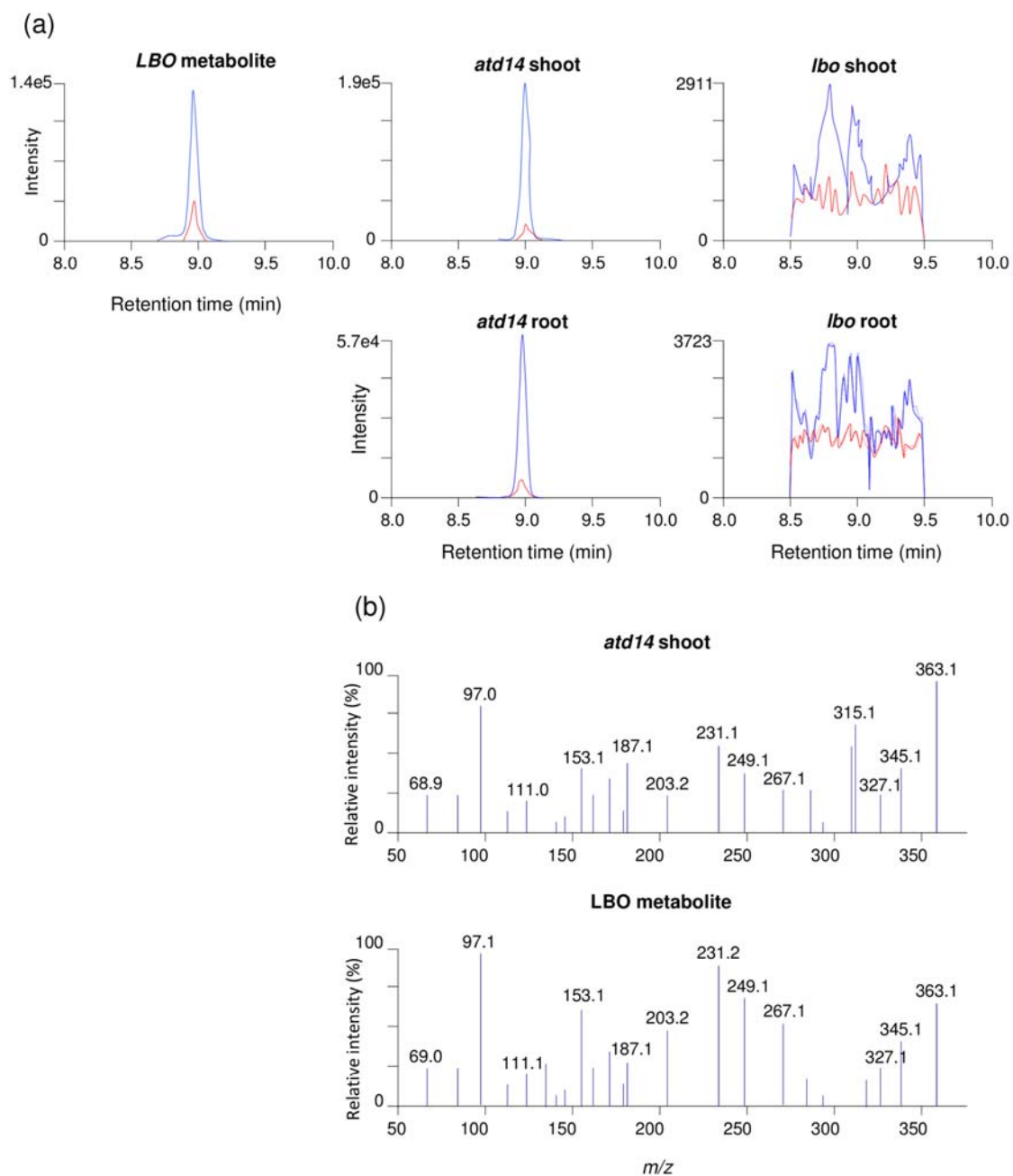
158 We previously described additional alleles of mutation in the *LBO* gene (Brewer et al. 2016).
159 *lbo-2* plants have a point mutation in the predicted catalytic domain and display significant
160 extra branching. *lbo-3* plants have a point mutation elsewhere in the gene and have a
161 branching phenotype that is much weaker than *lbo-2* (Brewer et al., 2016). LBO-2 and
162 LBO-3 proteins were produced in *E. coli* heterologous expression system and enzymatic
163 activities to produce 1'-HO-MeCLA were examined. The very low conversion of MeCLA to
164 1'-HO-MeCLA by LBO-2 enzyme activity (Fig. 5) relates well to the mutant shoot branching
165 phenotype. However, LBO-3 appears to have normal function in our assay (Fig. 5).

166

167 **Conversion of MeCLA into 1'-HO-MeCLA is conserved among different plant species**

168

169 Tomato, maize, and sorghum have one LBO homolog each and their recombinant LBO



170 proteins were expressed in *E. coli*. Not only *Arabidopsis* LBO but also the other LBO
171 proteins examined converted MeCLA into 1'-HO-MeCLA (Fig. 6), where the major reaction
172 product was CLA (Supplemental Fig. S1).

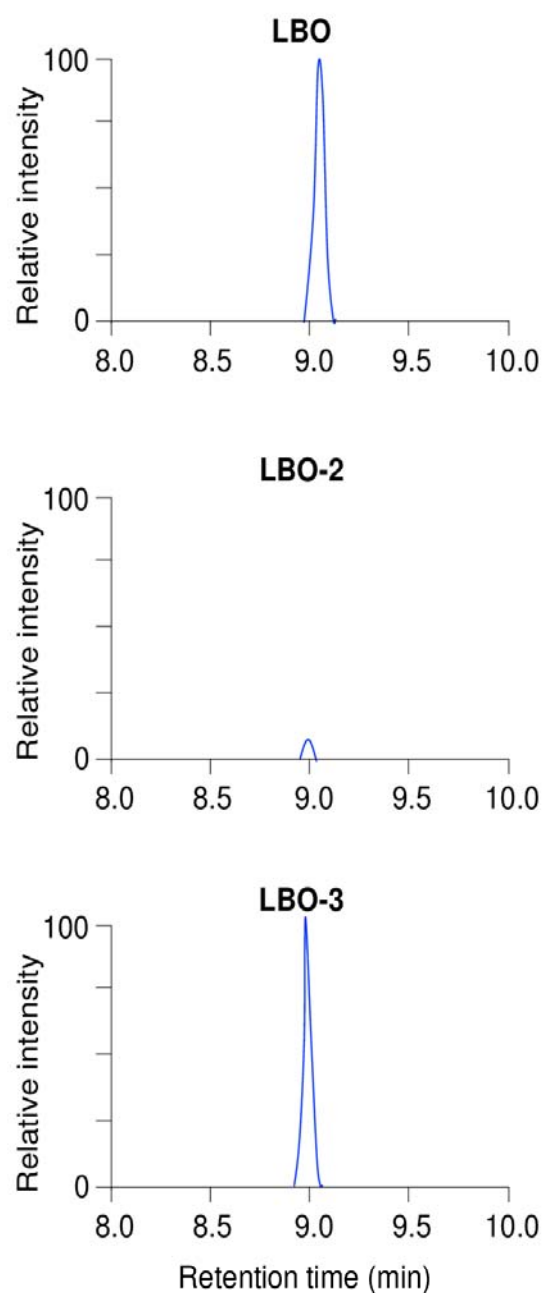


Figure 5. Production of 1'-HO-MeCLA is very low in LBO-2. MeCLA was incubated with each recombinant protein for 15 min and extracts were analyzed by LC-MS/MS. MRM chromatograms of 1'-HO-MeCLA (363.0/97.0; m/z in positive mode) are shown.

173 It is intriguing to test if LBO has an ability to produce canonical SLs or not. Tomato plants

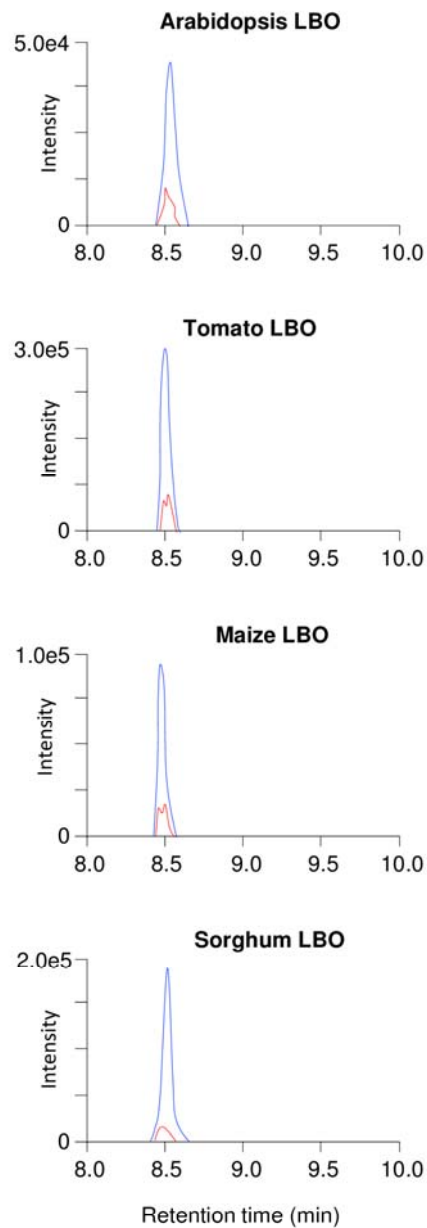


Figure 6. Conversion of MeCLA into 1'-HO-MeCLA is conserved among different plant species. MeCLA was incubated with each recombinant protein for 15 min and extracts were analyzed by LC-MS/MS. MRM chromatograms of 1'-HO-MeCLA (363.0/97.0; m/z in positive mode) are shown.

174 produce canonical SLs such as solanacol and orobanchol. Tomato MAX1 expressed in yeast
175 cannot produce canonical SLs from CL (Yoneyama et al., 2018). Accordingly, there is a
176 possibility that tomato LBO produces canonical SLs including solanacol and orobanchol.
177 However, tomato LBO produced neither solanacol nor orobanchol from MeCLA (Data not

178 shown). In addition, tomato LBO did not convert 4DO into solanacol or orobanchol, either
179 (data not shown). Similar results were obtained with sorghum or maize LBOs. Sorghum LBO
180 produced neither 5-deoxystrigol (5DS) nor sorgomol, two major canonical SLs of sorghum
181 (cv Hybrid), from MeCLA. Although it was proposed that sorgomol is produced from 5DS
182 (Motonami et al., 2013), LBO did not produce sorgomol from 5DS (data not shown). Maize
183 plants produce zealactone (Charnikhova et al., 2017; Xie et al., 2017) and zeapyranolactone
184 (Charnikhova et al., 2018), non-canonical SLs with unique structures. Maize LBO did not
185 produce these SLs from MeCLA (Data not shown).

186

187 **Endogenous non-canonical SLs in *Arabidopsis***

188

189 CYP711A2, one of rice MAX1 homologs, produces 4-deoxyorobanchol (4DO) via
190 18-HO-CLA from CL (Yoneyama et al., 2018). This suggests that not only 1'-HO-MeCLA
191 but also other HO-CL derivatives including HO-CLs, HO-CLAs, and HO-MeCLAs are
192 endogenous compounds in *Arabidopsis*, and some of them may be substrates for MAX1 and
193 LBO. Therefore, endogenous SLs in *atd14*, *max1* and *lbo* mutants were investigated in detail.
194 Synthetic standards of 2-, 3-, 4-, 16- and 18-HO-CL (Fig. 7) were prepared and used for
195 LC-MS/MS analyses. HO-CLAs (Fig. 7) were obtained by conversion of the corresponding
196 HO-CLs by MAX1 expressed in yeast. HO-MeCLAs (Fig. 7) were obtained by methylation
197 of the corresponding HO-CLAs with diazomethane.

198 Basal parts of *Arabidopsis* shoot were harvested when the shoot branching phenotype was
199 clearly observed (Supplemental Fig. S2). From *atd14* mutants, 3-, 4-, and 16-HO-CLs, 3-, 4-,
200 and 16-HO-CLAs, and 4- and 16-HO-MeCLAs, in addition to CL, CLA, and MeCLA, were
201 detected (Fig. 8).

202 3-, 4-, and 16-HO-CLs and CL were detected from basal parts of *max1* mutants (Fig. 8).

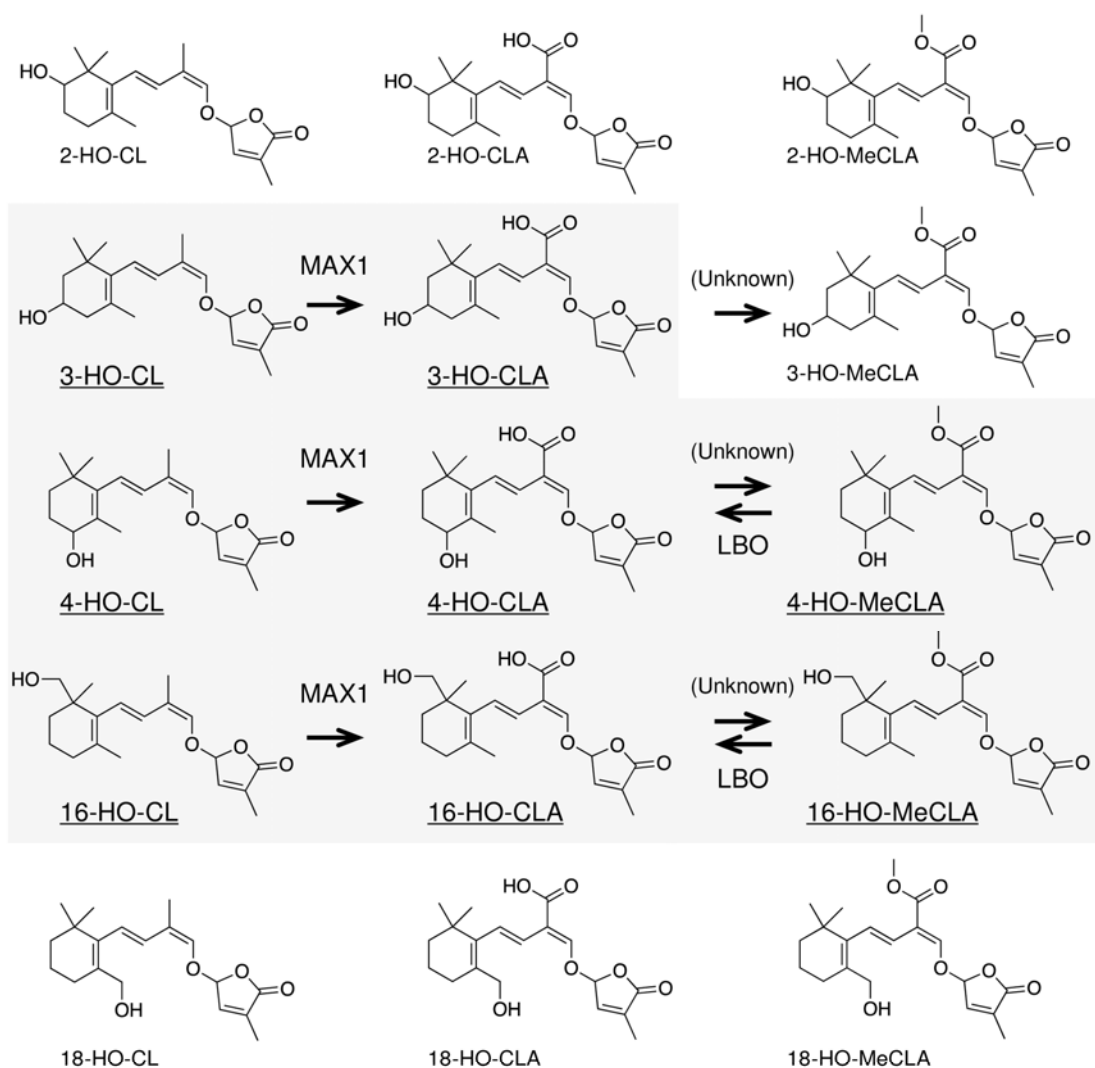


Figure 7. Structures of HO-CLs, HO-CLAs and HO-MeCLAs and a proposed strigolactone biosynthesis pathway in *Arabidopsis*. The present study shows that 3-, 4-, and 16-HO-CL derivatives are predominant and produced through MAX1 and LBO in *Arabidopsis*.

203 Although 3-, 4-, and 16-HO-CLAs were detected, even from Col-0 plants (Supplemental Fig.
 204 S3), these HO-CLAs were not detected in *max1* mutants (Fig. 8). By comparing peak areas of
 205 MRM chromatograms between *atd14* and *max1* mutants (Fig. 8), 3-, 4-, and 16-HO-CLs
 206 appeared to accumulate in *max1* mutants.
 207
 208 **4- and 16-HO-MeCLAs are potential substrates for LBO**

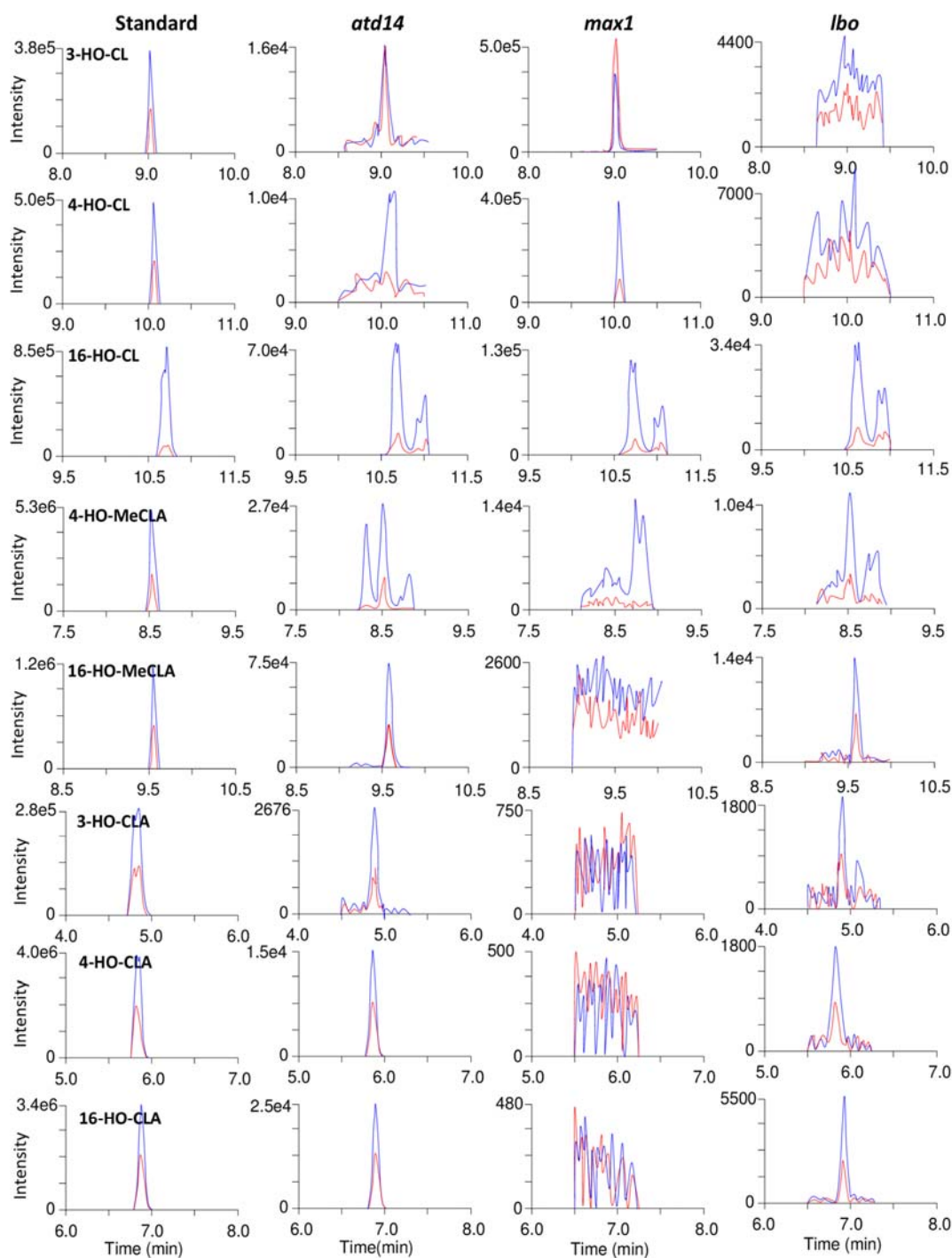


Figure 8. (a) HO-CLs and HO-MeCLAs are detected from ethyl acetate soluble fractions, and (b) HO-CLAs were from acidic fractions in basal parts of shoot tissues of *atd14* mutants, *max1* mutants, and *lbo* mutants. 3-, 4-, and 16-HO-CLs appeared to accumulate in *max1* mutants and 4- and 16-HO-MeCLA in *lbo* mutants. MRM chromatograms of 3-HO-CL (blue, 301.0/97.0; red, 319.0/205.0; *m/z* in positive mode), 4-HO-CL (blue, 301.0/97.0; red, 301.0/148.0; *m/z* in positive mode), 16-HO-CL (blue, 301.0/97.0; red, 301.0/189.0; *m/z* in positive mode), 4-HO-MeCLA (blue, 345.0/97.0; red, 345.0/216.0; *m/z* in positive mode), 16-HO-MeCLA (blue, 345.0/97.0; red, 363.0/97.0; *m/z* in positive mode), 3-, 4-, and 16-HO-CLA (blue, 347.0/113.0; red, 347.0/69.0; *m/z* in negative mode) are shown.

209

210 In addition to CL, CLA, and MeCLA, 16-HO-CL, 3-, 4-, 16-HO-CLAs, 4- and

211 16-HO-MeCLAs were found in *lbo* mutants (Fig. 8). MeCLA was found to be a substrate for
212 LBO (Brewer et al., 2016) and therefore these HO-MeCLAs also can be potential substrates
213 for LBO.

214 Then, these HO-CL derivatives were incubated with recombinant LBO proteins as potential
215 substrates. 4- and 16-HO-MeCLAs, but not other HO-CL derivatives were consumed by
216 LBO. Although we searched for LBO products of 4- and 16-HO-MeCLAs with the D-ring
217 fragment (m/z 97) as an indicator by LC-MS/MS, we could not find any candidates for LBO
218 products (Fig. 9). As in the case of MeCLA, the corresponding HO-CLA was detected as a
219 major reaction product.

220

221 **DISCUSSION**

222

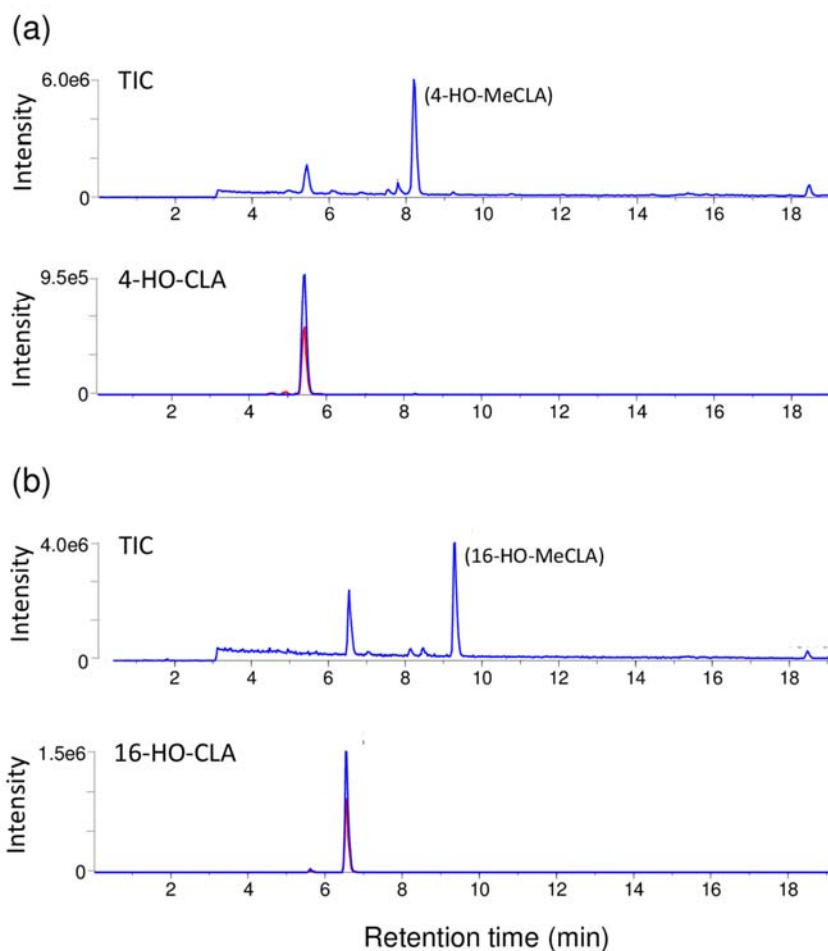


Figure 9. Recombinant LBO proteins convert 4-, and 16-HO-MeCLA mainly into the corresponding HO-CLAs. Each substrate was incubated for 15 min. The extracts were analyzed by LC-MS/MS with the D-ring fragment (m/z 97) as an indicator to identify the metabolites from each HO-CLA-fed LBO. Total Ion and MRM chromatograms of HO-CLAs (blue, 347.0/113.0; red, 347.0/69.0; m/z in negative mode) are shown.

223

224 The present study demonstrated that the structure of [MeCLA+16] Da is 1'-HO-MeCLA and
225 this LBO metabolite is endogenous in *Arabidopsis* tissues. 1'-HO-MeCLA was also produced
226 by MeCLA-fed maize, tomato and sorghum LBO proteins, suggesting that this conversion of
227 MeCLA into 1'-HO-MeCLA is highly conserved among different seed plant species.

228 Then the question arises whether 1'-HO-MeCLA is a strong shoot branching inhibitor or not.

229 So far, 1'-HO-MeCLA has not been examined for its effect on shoot branching. Unfortunately,
230 at this present time, the synthetic standard for 1'-HO-MeCLA is not available. As mentioned,
231 the yield of 1'-HO-MeCLA by LBO protein reaction is too low to obtain enough for shoot
232 branching assays. Since the substitution of 1'-HO-MeCLA is very unstable and could be
233 readily converted, it is possible that 1'-HO-MeCLA is a precursor for an unknown,
234 downstream shoot branching inhibitor(s) and a subsequent unknown enzyme(s) converts
235 1'-HO-MeCLA into the true shoot branching inhibitor(s). However, we cannot yet find any
236 candidate compounds that are likely to be derived from 1'-HO-MeCLA from *atd14* mutants
237 (data not shown). *LBO* was uncovered from transcriptomics (Brewer et al. 2016) and similar
238 methods recently led to the discovery that CYP722C from cowpea and tomato converts CLA
239 directly to orobanchol (Wakabayashi et al. 2019), and that a 2-oxoglutarate dependent
240 dioxygenase (2-OGD) from a nearby clade to *LBO* is involved in SL biosynthesis in *Lotus*
241 *japonicus* (Mori et al. 2020). We will continue reverse genetic and mass spectrometric
242 approaches to find related SL biosynthetic genes and shoot branching inhibitors. CLA seems
243 to be a key precursor for canonical SLs. We will test how LBO relates to CLA and canonical
244 SLs by identifying *lbo* mutants from plants that produce canonical SLs.

245 Worthy of attention here is that the LBO protein assay produces much more CLA from
246 MeCLA than 1'-HO-MeCLA. Such *O*-demethylations have been reported for 2-OGDs,
247 thebaine 6-*O*-demethylase and codeine *O*-demethylase, catalyzing *O*-demethylation in the
248 final steps of morphine biosynthesis (Hagel and Facchini, 2010). Therefore, we cannot
249 exclude the possibility that the main function of LBO is demethylation of MeCLA and that
250 1'-HO-MeCLA is just an intermediate for demethylation. This is somewhat difficult to
251 reconcile with our previous result that showed that CLA was detected from *lbo* mutants, but
252 not from its wild type (Brewer et al., 2016), indicating that CLA accumulates in *lbo* mutants.
253 As methyltransferase is proposed to be involved in conversion from CLA into MeCLA and

254 should be functional in *lbo* mutants. Thus, CLA would not be expected to accumulate in *lbo*
255 mutants unless the methyltransferase was somehow downregulated. Identification of the
256 methyltransferase will clarify the meaning of methylation and demethylation in the
257 production of shoot branching inhibitors.

258 *lbo-2* mutants with a point mutation in the predicted catalytic domain display extra shoot
259 branching. The present study demonstrated that recombinant LBO-2 protein is very weak at
260 converting MeCLA into 1'-HO-MeCLA (Fig. 5). In contrast, LBO-3 appears to have normal
261 function in our assay (Fig. 5). The shoot branching phenotype of *lbo-3* mutants with a point
262 mutation elsewhere in the gene is much weaker than *lbo-2*, and only just significantly more
263 than wild type (Brewer et al., 2016). It is possible that the protocol was not sensitive enough
264 to observe subtle defects in reaction efficiency. Alternatively, the LBO-3 mutation may reveal
265 an unknown protein functional or interaction domain at the mutation site, which only affects
266 its bioactivity *in planta*. It may be useful to test LBO and LBO-3 in combination with other
267 SL biosynthesis enzymes as they become discovered.

268 In addition to 1'-HO-MeCLA, other unstable non-canonical SLs were found in the basal
269 parts of shoot tissues (Fig. 8). So far, identification of SLs has been mainly conducted from
270 root tissues and this is the first report to show that SLs exist in basal parts of shoots of
271 *Arabidopsis*. There were no apparent differences in SL levels between the two tissues when
272 peak areas were compared (Fig. 4). In contrast, levels of SLs are very low or undetectable
273 from shoot of sorghum (Yoneyama et al., 2007) and rice plants (Umehara et al., 2010).
274 *Arabidopsis* could be quite particular in containing the same levels of SLs in the basal part of
275 shoot and root tissues. Perhaps this is because *Arabidopsis* is a non-host of AM fungi. Even
276 though *Arabidopsis* was reported to produce orobanchol (Goldwasser et al., 2008; Kohen et
277 al., 2011), a canonical SL that is widely distributed in plant kingdom (Yoneyama et al., 2008;
278 Yoneyama et al., 2011), we could detect neither orobanchol nor any other known canonical

279 SLs from *Arabidopsis* tissues (data not shown). Non-canonical SLs seem to be predominant
280 in *Arabidopsis* and may not be released into the soil because *Arabidopsis* does not need to
281 attract AM fungi to form a relationship with them. However, there are hints that SLs in
282 *Arabidopsis* may promote interaction with other beneficial soil fungi (Carvalhais et al. 2019).
283 So, there is likely much more to learn on that topic.

284 As summarized in Fig 7, MAX1 oxidizes C-19 methyl group to carboxylic acid not only in
285 CL, but also in HO-CLs in *Arabidopsis* plants. Baz et al. (2018) also detected 3-HO-CL from
286 rice *d14* mutant roots and demonstrated that 9-*cis*-3-HO- β -apo-10'-carotenal-fed to OsCCD8
287 is converted into 3-HO-CL. These results suggest that HO-CLs are also converted by MAX3
288 from HO-carotenal. The *Arabidopsis* MAX1 enzyme has the ability to convert 2-HO-CL and
289 18-HO-CL into respective HO-CLAs. However, these HO-CL derivatives could not be found
290 from *Arabidopsis* plants. It is intriguing why *Arabidopsis* produces such various and
291 particular HO-CL derivatives.

292

293 **CONCLUSION**

294

295 Deciphering the whole SL biosynthetic pathway and characterization of yet unidentified
296 biosynthetic intermediates is essential for devising new strategies to regulate the multiple
297 functions of SLs through manipulation of SL production and exudation, both quantitatively
298 and qualitatively. It should be noted that SL production and exudation vary with plant species
299 (even between cultivars or genotypes of the same plant species), growth conditions, and
300 growth stages. In the present study, we have unveiled the enzymatic functions of LBO and
301 MAX1 and their substrates and products downstream of CL in the SL biosynthetic pathway
302 in *Arabidopsis*. As most seed plant species sequenced so far contain a single *LBO* gene, and
303 the *LBO* gene lineage appears to have been derived deep in plant evolutionary history

304 (Walker et al., 2019), the biological function of LBO is likely to be highly conserved in the
305 plant kingdom.

306

307 **Materials and Methods**

308

309 **Plant material**

310

311 The *lbo-1* and *max1-4* were from our *Arabidopsis* laboratory stocks (Brewer et al., 2016) and
312 the *atd14-2* mutant was obtained from a TILLING project in the Columbia-0 (Col-0) ecotype.
313 To extract total RNAs, tomato (cv Ailisa Craig; Nomura et al., 2005), maize (cv B73;
314 Yoneyama et al., 2018) and sorghum (cv Hybrid; Yoneyama et al., 2008) were used.

315

316 **Chemicals**

317

318 3-, 4-, and 18-HO-CLs were synthesized as described previously (Mori et al. 2016; Baz et al.
319 2018). 2- and 16-HO-CLs were synthesized using the same strategy as the synthesis of 3- and
320 18-HO-CLs (Baz et al., 2018; Mori et al., 2016). The detailed synthesis will be published
321 elsewhere. 2-, 3-, 4-, 16- and 18-HO-CLA were obtained by MAX1 microsomal assay using
322 the corresponding HO-CLs. For this, MAX1 expressed in yeast (*Saccharomyces cerevisiae*)
323 was prepared as described previously (Abe et al., 2014, Yoneyama et al., 2018). 2-, 3-, 4-, 16-
324 and 18-HO-MeCLA were prepared by methylation of the corresponding HO-CLAs with
325 diazomethane.

326

327 **Synthesis of methyl-*d*₃ carlactonoate (1'-*d*₃-MeCLA) (Scheme S1)**

328

329 (*E*)-4-(2,6,6-Trimethylcyclohex-1-en-1-yl) but-3-enoic acid was synthesized as reported (Abe
330 et al., 2014). To a solution of the C₁₃-carboxylic acid (88.1 mg, 0.42 mmol) in acetone (2 mL),
331 K₂CO₃ (174 mg, 1.26 mmol) and methyl-*d*₃ iodide (305 mg, 131 μL, 2.1 mmol) were added.
332 The mixture was stirred at room temperature for 21 h under argon. After being concentrated
333 under nitrogen gas flow, the residue was dissolved with ether and water. The organic phase
334 was washed with water and dried over MgSO₄. Filtration and evaporation of the solvent
335 afforded C₁₃-carboxylic acid methyl-*d*₃ ester (82.3 mg, 0.37 mmol, 87%), which was pure
336 enough for the next reaction. Ester condensation of the methyl-*d*₃ ester (82.3 mg, 0.37 mmol)
337 with ethyl formate (98 mg, 106 μL, 1.32 mmol) by the use of sodium hydride (13.3 mg, 0.56
338 mmol) in *N,N*-dimethylformamide (1 mL) followed by alkylation with racemic
339 4-bromo-2-methyl-2-buten-4-olide (99 mg, 55 μL, 0.56 mmol) (Abe et al., 2014) provided
340 1'-*d*₃-MeCLA and ethyl carlactonoate (EtCLA, a transesterification product). Purification by
341 silica gel column chromatography (Kieselgel 60, Merck, *n*-hexane-ethyl acetate stepwise)
342 and semi-preparative HPLC (Inertsil SIL-100A, GL Sciences, 5% ethanol in *n*-hexane) gave
343 1'-*d*₃-MeCLA (2.5 mg, 0.0072mmol, 1.9%). **1'-*d*₃-MeCLA**: HR-ESI-TOF-MS *m/z*: 372.1855
344 [M+Na]⁺ (calcd. for C₂₀H₂₃D₃NaO₅⁺, *m/z*: 372.1861).

345

346 **Synthesis of methyl 18- *d*₃-carlactonoate (18-*d*₃-MeCLA) (Scheme S2)**

347

348 6,6-Dimethyl-2-(methyl-*d*₃)cyclohex-1-en-1-yl trifluoromethanesulfonate was synthesized as
349 reported (Tanaka et al., 2007). A mixture of the triflate (5.30 g, 19.3 mmol), triethylamine
350 (7.80 g, 10.7 mL, 77.2 mmol), methyl 3-butenolate (3.86 g, 4.11 mL, 38.6 mmol), and
351 bis(triphenylphosphine)palladium(II) dichloride (1.35 g, 1.92 mmol) in
352 *N,N*-dimethylformamide (50 mL) was stirred at 100°C for 17 h under argon. The reaction
353 mixture was cooled, quenched by pouring into 1 N HCl, and extracted with ether. The

354 organic phase was washed with brine and water, dried over MgSO₄, and concentrated in
355 vacuo. Purification by silica gel column chromatography (Kieselgel 60, Merck,
356 *n*-hexane-ether stepwise) gave crude methyl
357 (*E*)-4-(6,6-dimethyl-2-(methyl-*d*₃)cyclohex-1-en-1-yl)but-3-enoate (1.31 g, 5.8 mmol, 30%),
358 which was used for the next reaction without further purification. Ester condensation of the
359 deuterium-labeled ester (108 mg, 0.48 mmol) with methyl formate (86.4 mg, 89 μL, 1.44
360 mmol) by the use of sodium hydride (11.5 mg, 0.48 mmol) in *N,N*-dimethylformamide (1
361 mL) followed by alkylation with racemic 4-bromo-2-methyl-2-buten-4-olide (85 mg, 47 μL,
362 0.48 mmol) (Abe et al., 2014) provided 18-*d*₃-MeCLA. Purification by silica gel column
363 chromatography (Kieselgel 60, Merck, *n*-hexane-ethyl acetate stepwise), semi-preparative
364 normal-phase HPLC (Inertsil SIL-100A, GL Sciences, 5% ethanol in *n*-hexane) and
365 semi-preparative reversed-phase HPLC (InertSustain C18, GL Sciences, 85% acetonitrile in
366 water) gave 18-*d*₃-MeCLA (1.7 mg, 0.0049 mmol, 1.0%). **18-*d*₃-MeCLA**: HR-ESI-TOF-MS
367 *m/z*: 350.2058 [M + H]⁺ (calcd. for C₂₀H₂₄D₃O₅⁺, *m/z*: 350.2041).

368

369 Cloning

370

371 The primer sequences used are listed in Supporting Information TableS1. Total RNAs were
372 extracted from the shoots and roots of plant materials using an RNeasy Plant Mini Kit
373 (Qiagen, Hilden, Germany) and employed to synthesize single-strand cDNAs by a
374 SuperScript III First-Strand Synthesis System (Invitrogen, Waltham, MA, USA). PCR
375 amplification was performed using PrimeSTAR HS DNA polymerase (TAKARA Bio Inc.,
376 Kusatsu, Japan) with/without GC buffer for accurate amplification of GC rich targets. The
377 full-length cDNAs were cloned into the pENTR vector and then transferred to pET300 vector
378 by the Gateway system (Invitrogen). Recombinant plasmid DNA was transferred to

379 *Escherichia coli* strain Rosetta 2(DE3)pLysS (Novagen). At least four colonies for each
380 experiment were sequenced to check for errors in the PCR. Sequence alignment was
381 performed using MAC VECTOR software (Mac Vector Inc., Apex, NC, USA).

382

383 **Heterologous expression in *E. coli***

384

385 Heterologous expression of LBO in *E. coli* was carried out as described previously (Brewer
386 et al., 2016). Briefly, transformed colonies were grown in LB media (0.5% yeast extract, 1%
387 Bacto Tryptone, 1% NaCl) with carbenicillin (100 µg/mL) at 37 °C in a shaking incubator
388 (180 rpm) until the cell density reached an OD₆₀₀ of 0.5-0.8. After isopropyl
389 -D-1-thiogalactopyranoside (1 mM) was added, transformed *E. coli* were incubated at 20 °C
390 for 14-16 h. To prepare enzyme fractions, *E. coli* cells were collected by centrifugation of
391 10,000 x *g* for 1 min and suspended in 20 mM phosphate buffer (pH 7.4). The suspend cells
392 were mechanically lysed by using a high-pressure homogenizer (Emulsi Flex B15;
393 AVESTIN) and then, centrifuged at 15,000 x *g* for 5 min at 4°C.

394

395 **LBO enzyme assays and metabolite extraction**

396

397 Crude protein fraction (5 mL) was incubated with 4 mM 2-oxoglutarate, 0.5 mM iron
398 ascorbate, 5 mM ascorbic acid, and 12.5 µg of test substrates at 27°C for 20 min, similar to
399 the previous report (Brewer et al., 2016). The reaction mixture was extracted with 5 mL ethyl
400 acetate twice. The ethyl acetate soluble fraction was dried with sodium sulfate and
401 evaporated under nitrogen gas flow at 40°C with care not to completely dry. Crude extract
402 samples were kept at -20°C until LC-MS analysis.

403

404 **SL identification in *A. thaliana***

405

406 *Arabidopsis* seeds were sterilized in 1% sodium hypochlorite solution for 10 min and rinsed
407 with sterile water. Seeds were sown on agar (0.5% gellan gum with 1/2 Murashige and Skoog
408 medium and 1% sucrose), stratified at 4°C for 2 days, and grown for 10 days under a
409 photoperiod, 14 h: 10 h, light (150 mol m⁻² s⁻¹): dark, at room temperature. Then, healthy and
410 uniform seedlings were transplanted on soils [horticultural soil: vermiculite = 1: 2 (v/v)] and
411 further grown until branching phenotype became clear. Basal parts of shoot tissues were
412 harvested, extracted with ethyl acetate for at least 2 days and crude extracts were purified by
413 DEA and silica Sep-pack cartridge as reported previously (Brewer et al., 2016).

414

415 **LC-MS/MS analysis**

416

417 SLs were analyzed by LC-MS/MS as reported previously (Abe et al., 2014). Briefly,
418 LC-MS/MS analysis (MRM, multiple reaction monitoring and PIS, product ion scan) of
419 proton adduct ions was performed with a triple quadrupole/linear ion trap instrument
420 (QTRAP5500; AB Sciex, Old Connecticut Path Framingham, MA, USA) with an
421 electrospray source. HPLC separation was performed on a UHPLC (Nexera X2; Shimadzu)
422 equipped with an ODS column (Kinetex C18, 2.1 x 150 mm, 1.7 μm; Phenomenex) with a
423 linear gradient of 35% acetonitrile (0 min) to 95% acetonitrile (20 min). The column oven
424 temperature was maintained at 30°C.

425

426 **Supplemental Data**

427

428 **Supplemental Figure S1.** Detection of CLA from recombinant LBO proteins of various

429 plants.

430 **Supplemental Figure S2.** The number of shoot branching in *max1*, *lbo* and *atd14* mutants.

431 **Supplemental Figure S3.** Identification of HO-CLAs from Col-0.

432

433 **ACKNOWLEDGEMENTS**

434

435 We would like to thank Nozomi Nanai for technical assistance. This study was supported by
436 the Japan Science and Technology Research Promotion Program for Agriculture, Forestry,
437 Fisheries and Food Industry, the Japan Society for the Promotion of Sciences (KAKENHI
438 15K07093, 16K07618, 16K18560) and the Japan Science and Technology Agency PRESTO
439 (JPMJPR17QA).

440

441

442 **FIGURE LEGENDS**

443

444 **Figure 1.** Proposed strigolactone (SL) biosynthesis pathway in *Arabidopsis thaliana*. An
445 isomerase (AtD27) and two CCD enzymes (MAX3 and MAX4) convert β -carotene into
446 carlactone (CL), an endogenous common precursor for diverse SLs. CL is then oxidized by
447 cytochrome P450 (MAX1) to carlactonoic acid (CLA), which is converted into MeCLA by
448 unknown methyltransferase. The present study showed that 2-oxoglutarate-dependent
449 dioxygenase LBO converts MeCLA into 1'-HO-MeCLA, which is essential for regulating
450 shoot branching.

451

452 **Figure 2.** LBO converted [18-*d*₃]-MeCLA to [MeCLA+16+3] and [1'-*d*₃]-MeCLA to
453 [MeCLA+16+2]. To characterize the structure of [MeCLA+16], [18-*d*₃]-MeCLA (*Middle*)

454 and [1'-*d*₃] MeCLA (*Light*) were fed as substrates to recombinant LBO proteins and
455 incubated for 15 min. Products were identified by LC-MS/MS (MRM).

456

457 **Figure 3.** Most MeCLAs were converted to CLA. MeCLA was incubated with recombinant
458 LBO proteins for 15 min. The extracts were analyzed by LC-MS/MS (MRM).

459

460 **Figure 4.** 1'-HO-MeCLA was found from *atd14* shoot. Identification of endogenous
461 1'-HO-MeCLA in basal parts of shoot and root tissues was conducted. (a) MRM of
462 chromatograms (363.0/97.0; *m/z* in positive mode) of *atd14* mutants (*Middle*) and *lbo*
463 mutants (*Light*). (b) Product ion spectra derived from endogenous 1'-HO-MeCLA in basal
464 parts of shoot of *atd14* mutants.

465

466 **Figure 5.** Production of 1'-HO-MeCLA is very low in LBO-2. MeCLA was incubated with
467 each recombinant protein for 15 min and extracts were analyzed by LC-MS/MS. MRM
468 chromatograms of 1'-HO-MeCLA (363.0/97.0; *m/z* in positive mode) are shown.

469

470 **Figure 6.** Conversion of MeCLA into 1'-HO-MeCLA is conserved among different plant
471 species. MeCLA was incubated with each recombinant protein for 15 min and extracts were
472 analyzed by LC-MS/MS. MRM chromatograms of 1'-HO-MeCLA (363.0/97.0; *m/z* in
473 positive mode) are shown.

474

475 **Figure 7.** Structures of HO-CLs, HO-CLAs and HO-MeCLAs and a proposed strigolactone
476 biosynthesis pathway in *Arabidopsis*. The present study shows that 3-, 4-, and 16-HO-CL
477 derivatives are predominant and produced through MAX1 and LBO in *Arabidopsis*.

478

479 **Figure 8.** (a) HO-CLs and HO-MeCLAs are detected from ethyl acetate soluble fractions,
480 and (b) HO-CLAs were from acidic fractions in basal parts of shoot tissues of *atd14* mutants,
481 *max1* mutants, and *lbo* mutants. 3-, 4-, and 16-HO-CLs appeared to accumulate in *max1*
482 mutants and 4-, and 16-HO-MeCLA in *lbo* mutants. MRM chromatograms of 3-HO-CL (blue,
483 301.0/97.0; red, 319.0/205.0; *m/z* in positive mode), 4-HO-CL (blue, 301.0/97.0; red,
484 301.0/148.0; *m/z* in positive mode), 16-HO-CL (blue, 301.0/97.0; red, 301.0/189.0; *m/z* in
485 positive mode), 4-HO-MeCLA (blue, 345.0/97.0; red, 345.0/216.0; *m/z* in positive mode),
486 16-HO-MeCLA (blue, 345.0/97.0; red, 363.0/97.0; *m/z* in positive mode), 3-, 4-, and
487 16-HO-CLA (blue, 347.0/113.0; red, 347.0/69.0; *m/z* in negative mode) are shown.

488

489 **Figure 9.** Recombinant LBO proteins convert 4-, and 16-HO-MeCLA mainly into the
490 corresponding HO-CLAs. Each substrate was incubated for 15 min. The extracts were
491 analyzed by LC-MS/MS with the D-ring fragment (*m/z* 97) as an indicator to identify the
492 metabolites from each HO-CLA-fed LBO. Total Ion and MRM chromatograms of HO-CLAs
493 (blue, 347.0/113.0; red, 347.0/69.0; *m/z* in negative mode) are shown.

494

495

496 **LITERATURE CITED**

497

498

Parsed Citations

Abe S, Sado A, Tanaka K, Kisugi T, Asami K, Ota S, Kim HI, Yoneyama K, Xie X, Ohnishi T, et al (2014) Carlactone is converted to carlactonoic acid by MAX1 in Arabidopsis and its methyl ester can directly interact with AtD14 in vitro. Proc Natl Acad Sci USA 111: 18084-18089

Pubmed: [Author and Title](#)

Google Scholar: [Author Only Title Only Author and Title](#)

Akiyama K, Matsuzaki K, Hayashi H (2005) Plant sesquiterpenes induce hyphal branching in arbuscular mycorrhizal fungi. Nature 435: 824-827

Pubmed: [Author and Title](#)

Google Scholar: [Author Only Title Only Author and Title](#)

Agusti J, Herold S, Schwarz M, Sanchez P, Ljung K, Dun EA, Brewer PB, Beveridge CA, Sieberer T, Sehr EM, Greb T (2011) Strigolactone signaling is required for auxin-dependent stimulation of secondary growth in plants. Proc Natl Acad Sci USA 108: 20242-20247

Pubmed: [Author and Title](#)

Google Scholar: [Author Only Title Only Author and Title](#)

Al-Babili S and Bouwmeester H (2015) Strigolactones, a novel carotenoid derived plant hormone. Annual Review of Plant Biology 66: 161-186

Pubmed: [Author and Title](#)

Google Scholar: [Author Only Title Only Author and Title](#)

Alder A, Jamil M, Marzorati M, Bruno M, Vermathen M, Bigler P, Ghisla S, Bouwmeester H, Beyer P, Al-Babili S (2012) The path from β -carotene to carlactone, a strigolactone-like plant hormone. Science 335: 1348-1351

Pubmed: [Author and Title](#)

Google Scholar: [Author Only Title Only Author and Title](#)

Baz L, Mori N, Mi J, Jamil M, Kountche BA, Guo X, Balakrishna A, Jia KP, Vermathen M, Akiyama K, Al-Babili S (2018) 3-Hydroxycarlactone, a novel product of the strigolactone biosynthesis core pathway. Mol. Plant 11: 1312-1314

Pubmed: [Author and Title](#)

Google Scholar: [Author Only Title Only Author and Title](#)

Brewer PB, Yoneyama K, Filardo F, Meyers E, Scaffidi A, Frickey T, Akiyama K, Seto Y, Dun EA, Cremer JE et al (2016) LATERAL BRANCHING OXIDOREDUCTASE acts in the final stages of strigolactone biosynthesis in Arabidopsis. Proc Natl Acad Sci USA 113: 6301-6306

Pubmed: [Author and Title](#)

Google Scholar: [Author Only Title Only Author and Title](#)

Carvalhais LC, Rincon-Florez VA, Brewer PB, Beveridge CA, Dennis PG, Schenk PM (2019) The ability of plants to produce strigolactones affects rhizosphere community composition of fungi but not bacteria. Rhizosphere 9: 18-26

Pubmed: [Author and Title](#)

Google Scholar: [Author Only Title Only Author and Title](#)

Charnikhova TV, Gaus K, Lumbroso A, Sanders M, Vincken JP, De Mesmaeker A, Ruyter-Spira CP, Screpanti C, Bouwmeester HJ (2017) Zealactones. Novel natural strigolactones from maize. Phytochemistry 137: 123-131

Pubmed: [Author and Title](#)

Google Scholar: [Author Only Title Only Author and Title](#)

Charnikhova TV, Gaus K, Lumbroso A, Sanders M, Vincken J-P, De Mesmaeker A, Ruyter-Spira CP, Screpanti C, Bouwmeester HJ. (2018) Zeapyranolactone – A novel strigolactone from maize. Phytochemistry Letters 24: 172–178

Pubmed: [Author and Title](#)

Google Scholar: [Author Only Title Only Author and Title](#)

Cook CE, Whichard LP, Turner B, Wall ME, Egley GH (1966) Germination of witchweed (*Striga lutea* Lour.): isolation and properties of a potent stimulant. Science 154: 1189–1190

Pubmed: [Author and Title](#)

Google Scholar: [Author Only Title Only Author and Title](#)

Dor E, Joel DM, Kapulnik Y, Koltai H, Hershenhorn J (2011) The synthetic strigolactone GR24 influences the growth pattern of phytopathogenic fungi. Planta 234: 419-427

Pubmed: [Author and Title](#)

Google Scholar: [Author Only Title Only Author and Title](#)

Foo E and Davies NW (2011) Strigolactones promote nodulation in pea. Planta 234: 1073-1081

Pubmed: [Author and Title](#)

Google Scholar: [Author Only Title Only Author and Title](#)

Goldwasser Y, Yoneyama K, Xie X, Yoneyama K (2008) Production of strigolactones by *Arabidopsis thaliana* responsible for *Orobancha aegyptiaca* seed germination. Plant Growth Regulation 55: 21-28

Pubmed: [Author and Title](#)

Google Scholar: [Author Only Title Only Author and Title](#)

Gomez-Roldan V, Fermas S, Brewer PB, Puech-Pagès V, Dun EA, Pillot JP, Letisse F, Matusova R, Danoun S, Portais JC et al (2008) Strigolactone; inhibition of shoot branching. *Nature* 45: 189–194

Pubmed: [Author and Title](#)

Google Scholar: [Author Only](#) [Title Only](#) [Author and Title](#)

Ha CV, Leyva-Gonzalez MA, Osakabe Y, Tran UT, Nishiyama R, Watanabe Y, Tanaka M et al (2014) Positive regulatory role of strigolactone in plant response to drought and salt stress. *Proc Natl Acad Sci USA* 111: 851-856

Pubmed: [Author and Title](#)

Google Scholar: [Author Only](#) [Title Only](#) [Author and Title](#)

Hagel MJ and Facchini JP (2010) Dioxygenases catalyze the O-demethylation steps of morphine biosynthesis in opium poppy. *Nature Chemical Biology* 6: 273-275

Pubmed: [Author and Title](#)

Google Scholar: [Author Only](#) [Title Only](#) [Author and Title](#)

Kapulnik Y, Delaux PM, Resnick N, Mayzlish-Gati E, Winer S, Bhattacharya C et al (2011) Strigolactones affect lateral root formation and root-hair elongation in Arabidopsis. *Planta* 233: 209-216

Pubmed: [Author and Title](#)

Google Scholar: [Author Only](#) [Title Only](#) [Author and Title](#)

Kohlen W, Charnikhova T, Liu Q, Bours R, Domagalska MA, Beguerie S, Verstappen F, Leyser O, Bouwmeester H, Ruyter-Spira C (2011) Strigolactones are transported through xylem and play a key role in shoot architectural response to phosphate deficiency in nonarbuscular mycorrhizal host Arabidopsis. *Plant Physiology* 155: 974-987

Pubmed: [Author and Title](#)

Google Scholar: [Author Only](#) [Title Only](#) [Author and Title](#)

Mori N, Nishiuma K, Sugiyama T, Hayashi H, Akiyama K (2016) Carlactone-type strigolactones and their synthetic analogues as inducers of hyphal branching in arbuscular mycorrhizal fungi. *Phytochemistry* 130: 90-98

Pubmed: [Author and Title](#)

Google Scholar: [Author Only](#) [Title Only](#) [Author and Title](#)

Mori N, Nomura T, Akiyama K (2020) Identification of two oxygenase genes involved in the respective biosynthesis pathways of canonical and non-canonical strigolactones in *Lotus japonicas*. *Planta* 251: 40

Pubmed: [Author and Title](#)

Google Scholar: [Author Only](#) [Title Only](#) [Author and Title](#)

Nomura T, Kushihiro T, Yokota T, Kamiya Y, Bishop GJ, Yamaguchi S (2005) The last reaction producing brassinolide is catalyzed by cytochrome P-450s, CYP85A3 in tomato and CYP85A2 in Arabidopsis. *The Journal of Biological Chemistry* 280: 17873-17879

Pubmed: [Author and Title](#)

Google Scholar: [Author Only](#) [Title Only](#) [Author and Title](#)

Nomura T, Magome H, Hanada A, Takeda-Kamiya N, Mander LN, Kamiya Y, Yamaguchi S (2013) Functional analysis of Arabidopsis CYP714A1 and CYP714A2 reveals that they are distinct gibberellin modification enzymes. *Plant Cell physiology* 54: 1837-1851

Pubmed: [Author and Title](#)

Google Scholar: [Author Only](#) [Title Only](#) [Author and Title](#)

Ruyter-Spira C, Kohlen W, Charnikhova T, Zeijl A, Bezouwen L, Ruijter N, Cardoso C, Lopez-Raez et al (2011) Physiological effects of the synthetic strigolactone analog GR24 on root system architecture in Arabidopsis: another belowground role for strigolactones? *Plant Physiol* 155: 721-734.

Pubmed: [Author and Title](#)

Google Scholar: [Author Only](#) [Title Only](#) [Author and Title](#)

Seto Y, Sado A, Asami K, Hanada A, Umehara M, Akiyama K, Yamaguchi S (2014) Carlactone is an endogenous biosynthetic precursor for strigolactones. *Proc Natl Acad Sci USA* 111: 1640-1645

Pubmed: [Author and Title](#)

Google Scholar: [Author Only](#) [Title Only](#) [Author and Title](#)

Soto MJ, Fernandez-Aparicio M, Castellanos-Morales V, Garcia-Garrido JA, Delgado MJ, Vierheilig H (2010) First indications for the involvement of strigolactone on nodule formation in alfalfa (*Medicago sativa*). *Soil Biol Biochem* 42: 383-385

Pubmed: [Author and Title](#)

Google Scholar: [Author Only](#) [Title Only](#) [Author and Title](#)

Tanaka K, Struts VA, Krane S, Fujioka N, Salgado GFJ, Martínez-Mayorga K, Brown MF, Nakanishi K (2007) Synthesis of CD3-Labeled 11-cis-Retinals and Application to Solid-State Deuterium NMR Spectroscopy of Rhodopsin. *Bull. Chem. Soc. Jpn.* 80: 2177–2184.

Pubmed: [Author and Title](#)

Google Scholar: [Author Only](#) [Title Only](#) [Author and Title](#)

Ueda H, Kusaba M (2015) Strigolactone regulates leaf senescence in concert with ethylene in Arabidopsis. *Plant Physiol* 169: 138–147

Pubmed: [Author and Title](#)

Google Scholar: [Author Only](#) [Title Only](#) [Author and Title](#)

Umehara M, Hanada A, Yoshida S, Akiyama K, Arite T, Takeda-Kamiya N, Magome H, Kamiya Y, Shirasu K, Yoneyama K et al (2008) Inhibition of shoot branching by new terpenoid plant hormones. *Nature* 455: 195–200

Pubmed: [Author and Title](#)

Google Scholar: [Author Only](#) [Title Only](#) [Author and Title](#)

Wakabayashi T, Hamana M, Mori A, Akiyama R, Ueno K, Osakabe K, Osakabe Y, Suzuki H, Takikawa H, Mizutani M, Sugimoto Y (2019) Direct conversion of carlactonoic acid to orobanchol by cytochrome P450 CYP722C in strigolactone biosynthesis. *Science Advances* 5: eaax9067

Pubmed: [Author and Title](#)

Google Scholar: [Author Only](#) [Title Only](#) [Author and Title](#)

Walker CH, Siu-Ting K, Taylor A, O'Connel MJ, Bennett T (2019) Strigolactone synthesis is ancestral in land plants, but canonical strigolactone signaling is a flowering plant innovation. *BMC Biology* 17:70

Pubmed: [Author and Title](#)

Google Scholar: [Author Only](#) [Title Only](#) [Author and Title](#)

Xie X, Kisugi T, Yoneyama K, Nomura T, Akiyama K, Uchida K, Yokota T, McErlean CSP, Yoneyama K (2017) Methyl zealactonoate, a novel germination stimulant for root parasitic weeds produced by maize. *J Pesticide Science* 42: 58-61

Pubmed: [Author and Title](#)

Google Scholar: [Author Only](#) [Title Only](#) [Author and Title](#)

Yamada Y, Furusawa S, Nagasaka S, Shimomura K, Yamaguchi S, Umehara M (2014) Strigolactone signaling regulates rice leaf senescence in response to a phosphate deficiency. *Planta* 240: 399-408

Pubmed: [Author and Title](#)

Google Scholar: [Author Only](#) [Title Only](#) [Author and Title](#)

Yoneyama K, Xie X, Sekimoto H, Takeuchi Y, Ogasawara S, Akiyama K, Hayashi H, Yoneyama K (2008) Strigolactones, host recognition signals for root parasitic plants and arbuscular mycorrhizal fungi, from Fabaceae plants. *New Phytol* 179: 484-494

Pubmed: [Author and Title](#)

Google Scholar: [Author Only](#) [Title Only](#) [Author and Title](#)

Yoneyama K, Xie X, Kisugi T, Nomura T, Sekimoto H, Yokota T, Yoneyama K (2011) Characterization of strigolactones exuded by Asteraceae plants. *Plant Growth Regulation* 65: 495-504

Pubmed: [Author and Title](#)

Google Scholar: [Author Only](#) [Title Only](#) [Author and Title](#)

Yoneyama K, Mori N, Sato T, Yoda A, Xie X, Okamoto M, Iwanaga M, Ohnishi T, Nishiwaki H et al (2018) Conversion of carlactonoic acid is a conserved function of MAX1 homologs in strigolactone biosynthesis. *New Phytol* 218: 1522-1533

Pubmed: [Author and Title](#)

Google Scholar: [Author Only](#) [Title Only](#) [Author and Title](#)